

# Dams induced stage–discharge relationship variations in the upper Yangtze River basin

Xuefei Mei, Zhijun Dai, Wen Wei and Jinjuan Gao

## ABSTRACT

Although stage–discharge relationships are crucial for discharge estimations and hydrological analyses, few efforts have been taken to assess their temporal alterations in the context of dam regulation. Here, the upper Yangtze River basin serves as an example to demonstrate the influence of hydraulic structures on stage–discharge relationships evolution. Daily records of water level and river discharge from 1950 to 2013 at Yichang hydrometric station were grouped and analyzed.

Back-propagation artificial neural network was used to model the stage–discharge relationships. The obtained curves revealed substantial shifts since the Gezhouba Dam (GD) and Three Gorges Dam (TGD) were put into practice sequentially. In low flow scenarios, the decline of water levels due to GD and TGD regulation were variable with river discharge, whereas in normal flow scenarios, the rating curves indicate equilibrium state with almost the same slopes regardless of GD and TGD influence. In high flow scenarios, the rating curves representing natural condition, GD, and TGD regulation intersect with each other. Moreover, the detected changes in stage–discharge relationship were mainly in response to dam regulation, channel erosion and sand exploitation, while irrelevant to precipitation variability. The contribution of sand mining, GD regulation, and TGD regulation on rating curve variations at Yichang station were 36%, 11%, and 53%, respectively.

**Key words** | artificial neural network, dam, rating curve, upper Yangtze River

Xuefei Mei  
Zhijun Dai (corresponding author)  
Wen Wei  
Jinjuan Gao  
State Key Laboratory of Estuarine & Coastal  
Research,  
East China Normal University,  
Shanghai,  
China  
E-mail: zjdai@sklec.ecnu.edu.cn

## INTRODUCTION

The relationship between stage and discharge is of considerable significance to understanding river behaviors (Sudheer & Jain 2003; Al-Abadi 2014). A reliable stage–discharge relationship (also known as rating curve) is the fundamental component for stream-flow estimation and forecasting. Such information is vital for coping with extreme events, such as floods and droughts. Over the past century, significant variations in river hydrology and morphology have been reported around the world as a result of climate change and human activities, which further affect the relationship between water level and river flow (Dai *et al.* 1998; Dettlinger & Diaz 2000; Labat *et al.* 2004; Milly *et al.* 2005; Milliman *et al.* 2008; Naik & Jay 2011). In such a situation, the former rating curves that were free from outside interferences are no longer feasible. Consequently, there is a need

to re-evaluate the stage–discharge relationship by taking account of environmental changes, especially human activities.

A number of techniques have been applied to model river stage–discharge relationships (Tawfik *et al.* 1997; Birkhead & James 1998; Jain & Chalisgaonkar 2000; Kisi & Cobaner 2009). The conventional approaches, including power-law function and multiple linear regression equation, approximate the best fitting curve for a particular gauging station through the observed water level and the passing discharge (Kisi & Cobaner 2009). It is noteworthy that the traditional methods link the measured water level unequivocally to a discharge, which disregard the hysteretic behavior due to effects of unsteadiness and back water (Tawfik *et al.* 1997; Wolfs & Willems 2014). To overcome significant

doi: 10.2166/nh.2015.010

unsteadiness effects, Jones's formula and its variations are recommended (Birkhead & James 1998; Perumal *et al.* 2004; Petersen-Øverleir 2006). However, these approaches neglect variable backwater effects. In recent years, a number of computing techniques have been proposed for constructing rating curves, including artificial neural network (ANN), Bayesian technics, genetic programming and fuzzy theory (Jain & Chalisgaonkar 2000; Moyeed & Clarke 2005; Guven & Aytek 2009; Shrestha & Simonovic 2010). As compared to the conventional approaches, these computing techniques produce quite satisfactory results and allow for back water, unsteadiness, and channel modification effects.

Although great attempts have been made to effectively relate the stage to discharge, few works address the impacts of dam regulations on stage-discharge relationships. Recently, Gordon & Meentemeyer (2006) examined the rating curves for a stream system in northern California, and indicated significant changes in channel morphology between the pre- and post-dam periods. Wang *et al.* (2013) established yearly stage-discharge rating curves for the Three Gorges Dam's (TGD) downstream during 2004–2012, and suggested that channel geometrics reshaped stage-discharge rating curves. More recently, Zhang *et al.* (2015) reconstructed stage-discharge relationships for the Pearl River Delta, and pointed out that water stages became lower in terms of the same amount of discharge due to sand excavation. Most previous works linked the water level measurements unequivocally to discharge records when investigating the influence of dam on stage-discharge relationships, which disregarded hysteresis of rating curves.

Over the past century, around 97,000 dams have been constructed in China, with a total storage of 810.410 billion m<sup>3</sup>, which makes China the world's largest dam builder (MWR 2013). Combined with climate change, this hydraulic engineering suggests significant effects on river behaviors over the country (Lu 2005; Chen *et al.* 2009; Yang & Tian 2009; Jiang *et al.* 2011; Zhang *et al.* 2012; Zhao *et al.* 2013). The Yangtze River basin is the most prominent example of intensive hydraulic engineering under the scenario of climate change, and thus has attracted considerable concern (Zhang *et al.* 2008a). The modifications in water resources have been documented in terms of discharge (Dai *et al.*

2008; Xu *et al.* 2008), water level (Zhang *et al.* 2006a; Wang *et al.* 2013), base-flow (Dai *et al.* 2010), sediment (Xu *et al.* 2006b; Yang *et al.* 2006; Zhang *et al.* 2006b; Dai & Liu 2013), and rating curves of discharge versus sediment (Xu & Milliman 2009). In spite of considerable research on hydrology changes in the Yangtze River basin, most of the previous works focused solely on an individual hydrological component, which failed to examine the effects of changing environment on integrated index, such as stage-discharge relationship.

Thereafter, the aims of this research include: (1) to set up stage-discharge rating curves for Yichang station in various flow scenarios based on the most advanced ANN theory; (2) to detect changes of stage-discharge relationship over the period 1950–2013, during which Gezhouba Dam (GD) and TGD were constructed; (3) to link the rating curve variations to human activities and climate change in the river basin, including dam regulation, sand exploitation, and precipitation variation; and (4) to quantify the effects of individual factors (sand mining, GD operation, and TGD operation) on rating curves.

## STUDY AREA

The Yangtze River (91 °E–122 °E, 25 °N–35 °N) is the third longest river in the world and the longest in Asia, with a length of over 6,300 km. It originates from the Qinghai-Tibet Plateau, and reaches the East China Sea near Shanghai. The Yangtze River covers 20% of China with a total drainage area of 1.8 million km<sup>2</sup>. Generally, the Yangtze River is partitioned into three sub-reaches (upper, middle, and lower reaches) according to its hydrologic and geomorphologic characteristics (Xu *et al.* 2006a). The three terms are referred to as the reaches above Yichang, from Yichang to Hukou, and from Hukou to the estuary, respectively.

The upper Yangtze River (Figure 1) covers a length of 4,504 km and a drainage area of around 1.0 million km<sup>2</sup> (Zhang *et al.* 2008b). The reach mainly goes through mountains and plateaus, with an average riverbed gradient of 1.1‰ (Yang *et al.* 2007). Jinshajiang, Jialingjiang, Minjiang and Wujiang rivers are major tributaries that flow into the main stream of the upper Yangtze River. Being subjected

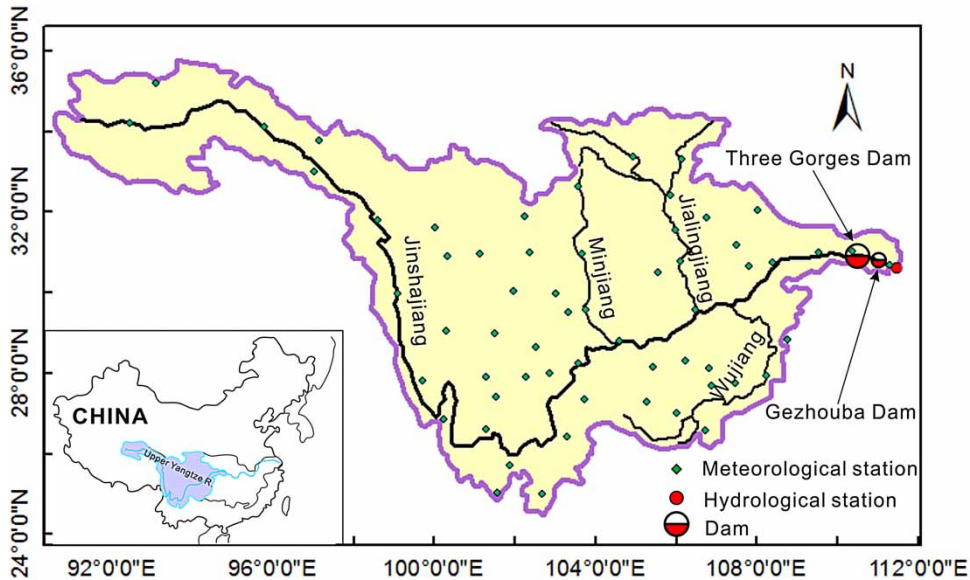


**Figure 1** | Map of the upper Yangtze River.

to Asian monsoon circulation, the upper Yangtze River experiences a cold and dry winter, and a warm and wet summer (Chen *et al.* 2007). The annual precipitation over the upper catchment ranges from 150 to 1,000 mm, with a mean value of 809 mm, over 60% of which falls between June and September.

The Yangtze River is controlled by around 50,000 reservoirs, among them the most notable examples being GD and TGD from the upstream basin (Yang *et al.* 2005). GD is the first dam that crosses the main stream of the Yangtze River. As a part of the Three Gorges project, GD aims to re-regulate the tail water from the TGD and improve the navigation condition between the two dams. GD was put into use in 1981 and was completed in 1988. TGD is the largest hydroelectric engineering project in the world. Three major functions of TGD are flood control, navigation, and hydropower generation. The TGD dam began to retain water and sediment in June 2003 and was completed in 2009. Characteristics of the two dams are provided in Table 1.

Yichang hydrometric station, located about 6 km downstream of GD and 44 km downstream of TGD, is the outflow control station of the upper Yangtze River. Yichang station covers an area of  $1.1 \times 10^6 \text{ km}^2$ , with a mean yearly water discharge of  $439 \times 10^9 \text{ m}^3$  (Dai *et al.* 2014).

## DATA AND METHODS

### Data collection

Daily records of discharge, water level, and sediment load from 1950 to 2013 at Yichang hydrometric station are collected from the Changjiang Water Resources Commission (CWRC), China ([www.cjh.com.cn](http://www.cjh.com.cn)). In addition to the above hydrological data, the precipitation records of 60 meteorological stations during 1950–2013 over the upper Yangtze River basin have been collected from the China Meteorological Administration. The measurements related to the Yichang cross section during 1970–2013 are collected from CWRC.

**Table 1** | Main technical parameters of GD and TGD

River	Dam	Dam height (m)	Dam length (m)	Reservoir areas (km <sup>2</sup> )	Reservoir capacity (10 <sup>6</sup> m <sup>3</sup> )	Initial operation year
Yangtze	GD	70	2,606	79.3	1,580	1981
	TGD	185	3,035	1,084	39,300	2003

For purposes of analysis, the data samples at Yichang station are divided into three segments according to the construction of GD (1981) and TGD (2003), namely Phase 1 from 1950 to 1980, Phase 2 from 1981 to 2002 and Phase 3 from 2003 to 2013. The 64 study years (from 1950 to 2013) are a mix of dry, normal, and wet years. Following Lloyd-Hughes & Saunders (2002), the ratio between yearly discharge and the average annual discharge ( $r$ ) is used to categorize the hydrological years, with breaking points of 1.2 and 0.85, respectively. The wetness of each year is described in Table 2. Dams affect the downstream hydrologic regime differently at high, normal, and low flow scenarios, therefore some studies have classified the flows into groups to fully quantify the influence of dam on discharge and water level (Shin 2007; McManamay 2014). TGD, as the largest dam in the world, dramatically modifies the downstream flow regime in flood and dry seasons and results in ‘no flood in the flood season, no drought in the dry season’ (Dai *et al.* 2008; Mei *et al.* 2015). Accordingly, the daily flow data are further categorized into three intervals according to the upper Yangtze River’s hydraulic conditions, with separating points of 7,000 and 20,000 m<sup>3</sup>/s. Hence, nine types of data set are defined, as shown in Figure 2.

## Methods

### Change tests

In statistical data analysis, change tests (trend test and abrupt change test) are necessary and critical steps. The purpose of trend test is to determine whether a data series has a gradual increase or decrease with time,

**Table 2** | Illustration of wetness years

Period	Wet year	Normal year	Dry year
1950–1980	1954; 1964; 1968; 1974	1950–1953; 1955–1958; 1960–1963; 1965– 1967; 1970–1972; 1973; 1975–1980	1959; 1969; 1972
1981–2002	1998	1981–1993; 1995–1996; 1999–2002	1994; 1997
2003–2013	2005; 2012	2003–2004; 2007–2010; 2013	2006; 2011

whereas the purpose of abrupt change test is to detect if there is a time at which a sudden jump occurs in a set of data. In the present study, the Mann–Kendall (MK) test is applied for analyzing trend while the standard normal homogeneity (SNH) test is used for detecting abrupt change in the hydrological time series, and these are described in detail by Yue *et al.* (2002) and Khaliq & Ouarda (2007), respectively.

### ANN

ANN, originating from the idea of human brain processes, has strong learning, reserving, and concluding abilities. It is an efficient tool for modeling and forecasting the complicated nonlinear relationship between input and output of a system (Hsu *et al.* 1995; Bourquin *et al.* 1998). Compared with the simple rating curve approach, ANN is less sensitive to the error term assumptions. However, despite their satisfactory performances in the reported studies, ANN models are prone to uncertainties due to their ‘black box’ nature and random construction of training set (Talebizadeh *et al.* 2009). Therefore, it is necessary to validate ANN models and check their accuracies prior to their implementation.

This study employs the feed-forward ANN with the back-propagation training algorithm (Rojas 1996), which includes an input layer, a hidden layer, and an output layer (shown in Figure 3). There are several neurons on each layer. Stimulation is applied to the inputs of the first layer, and signals propagate through the hidden layer to the output layer through connection links. Each link between neurons has an associated weight value that represents its connection strength. Such a three-layered ANN adjusts the weights according to the strength of the signal in the connection and the sum of the error. The cycle is repeated until the overall error for all data sets is minimal. In this study, water level records are considered as inputs while the discharge is predicted at the outlet.

### Thiessen polygon method

As a classical weighted mean method, Thiessen polygon method transfers the observed point precipitation into

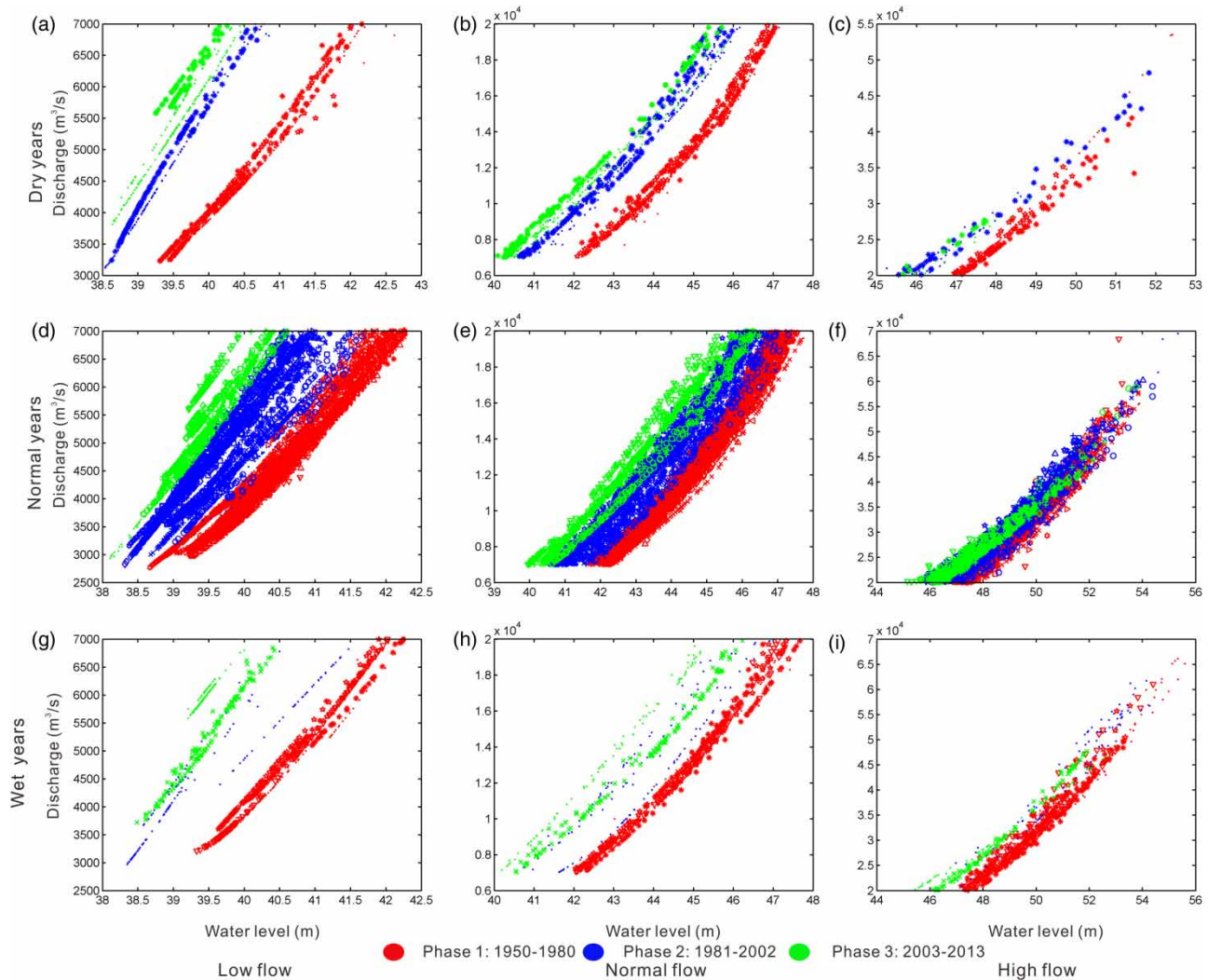


**Figure 2** | Daily water level and discharge at Yichang during 1950 to 2013.

areal average precipitation by the following function (Fielder 2003):

$$P = \sum_{i=1}^n w_i P_i \quad (1)$$

$$w_i = \frac{A_i}{A} \quad (2)$$

where  $P$  is areal average precipitation,  $P_i$  is point precipitation,  $w_i$  is Thiessen weight,  $A_i$  is area represented by the station,  $A$  is total watershed area,  $n$  is the number of precipitation stations over the basin.

## RESULTS

### Change in water level and discharge

For the purpose of stage–discharge relationship analysis, change tests are applied to the individual water level and discharge series first, including annual minimum discharge ( $Q_{\min}$ ), annual mean discharge ( $Q_{\text{mean}}$ ), annual maximum discharge ( $Q_{\max}$ ), annual minimum water level ( $h_{\min}$ ), annual mean water level ( $h_{\text{mean}}$ ), and annual maximum water level ( $h_{\max}$ ).

From the MK test results, it is noted that all data series for the period 1950–2013 exhibit significant downtrends at

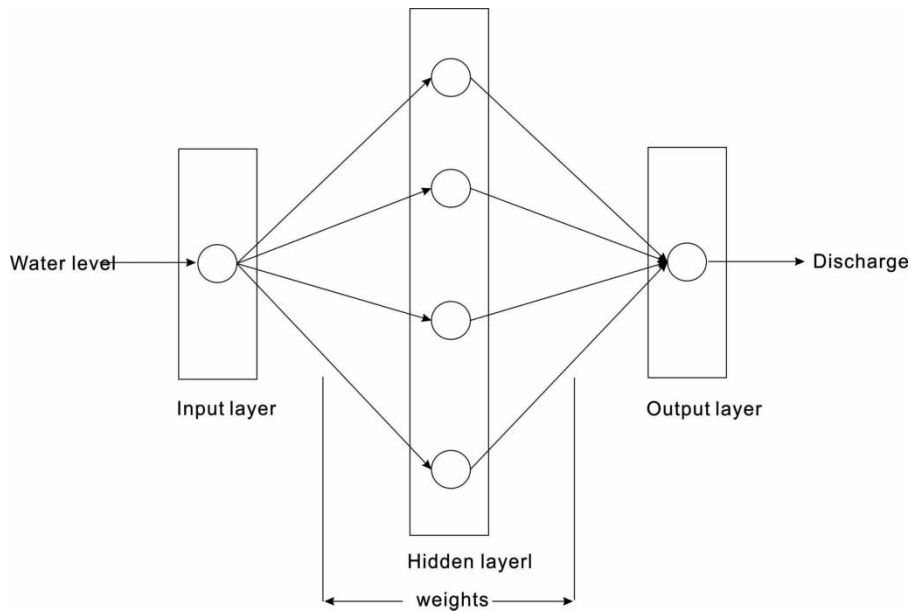


Figure 3 | Structure of three-layered feed-forward back-propagation ANN.

a 0.05 significance level, except for  $Q_{\min}$  which presents an upward trend (Table 3).

The results of the SNH test are also listed in Table 3, and indicate abrupt changes for all data sets at a significant level of 5%. It is shown that change points are located in two time intervals. For  $Q_{\min}$ ,  $Q_{\text{mean}}$ ,  $Q_{\text{max}}$ ,  $h_{\text{mean}}$ , and  $h_{\text{max}}$ , the shifts occurred around 2003, while for  $h_{\min}$ ,  $h_{\text{mean}}$ , and  $h_{\text{max}}$  significant changes were indicated around 1981. It is worth noting that the  $h_{\text{max}}$  and  $h_{\text{mean}}$  series detect two mutations, respectively, around 1981 and 2003.

### Training and variation of ANN model

For evaluating the effectiveness of ANN model on rating curves generation at Yichang station, daily discharge and associated water level are divided into two sets according to DUPLEX data splitting method (Snee 1977). One set is employed for training, while the other one is used for verification. The performance of ANN model during the training and validation stages are presented in Table 4. Two goodness-of-fit measures, correlation coefficient ( $R$ ), and root mean

Table 3 | Change test report for discharge and water level series

Parameter	Mann-Kendall test			Standard normal homogeneity test		
	$Z_{MK}$	$Z$	Trend	$T_0$	$T$	Shift year
Annual minimum discharge	2.67	1.96	Up	43.30	8.72	2006
Annual mean discharge	-2.24	1.96	Down	9.95	8.72	2004
Annual maximum discharge	-3.30	1.96	Down	12.40	8.72	2004
Annual minimum water level	-5.93	1.96	Down	39.00	8.72	1977
Annual mean water level	-7.2	1.96	Down	36.04/24.80	8.72	1985/2004
Annual maximum water level	-3.04	1.96	Down	9.05/9.33	8.72	1983/2004

**Table 4** | Performance indices of ANN for different scenarios in training and validation stages

Scenario	Training		Validation	
	R	RMSE (m <sup>3</sup> /s)	R	RMSE (m <sup>3</sup> /s)
Wet year (50–80) low flow	0.99	130	0.99	137
Wet year (50–80) normal flow	0.99	393	0.99	399
Wet year (50–80) high flow	0.99	1,585	0.98	1,772
Wet year (81–02) low flow	0.98	233	0.98	223
Wet year (81–02) normal flow	0.95	1,029	0.9	1,541
Wet year (81–02) high flow	0.98	2,288	0.99	1,854
Wet year (03–13) low flow	0.88	333	0.88	335
Wet year (03–13) normal flow	0.97	884	0.97	973
Wet year (03–13) high flow	0.99	1,032	0.99	1,054
Normal year (50–80) low flow	0.99	167	0.99	172
Normal year (50–80) normal flow	0.99	553	0.99	535
Normal year (50–80) high flow	0.98	1,481	0.98	1,607
Normal year (81–02) low flow	0.91	407	0.91	401
Normal year (81–02) normal flow	0.98	844	0.97	863
Normal year (81–02) high flow	0.98	1,664	0.97	1,771
Normal year (03–13) low flow	0.94	269	0.94	288
Normal year (03–13) normal flow	0.98	735	0.98	707
Normal year (03–13) high flow	0.98	1,209	0.98	1,235
Dry year (50–80) low flow	0.99	111	0.99	126
Dry year (50–80) normal flow	0.99	347	0.99	376
Dry year (50–80) high flow	0.99	854	0.97	1,436
Dry year (81–02) low flow	1	84	1	101
Dry year (81–02) normal flow	0.99	452	0.99	442
Dry year (81–02) high flow	0.99	722	1	655
Dry year (03–13) low flow	0.95	232	0.96	221
Dry year (03–13) normal flow	0.99	420	0.99	389
Dry year (03–13) high flow	0.98	546	0.99	416

square error (RMSE) are used to evaluate the capability of the predictions over the observations. The calculated *R* values between predictions and observations range from 0.88 to 1 during the validation period as well as training period, which show statistically significant correlation ( $p < 0.001$ ). Therefore, the ANN model is capable of capturing good simulation performance at Yichang station. Moreover, the RMSE values are located in the range of 84–2,288 m<sup>3</sup>/s and 101–1,854 m<sup>3</sup>/s for training and validation stages, respectively.

### Stage–discharge relationship

As Figure 2 indicates, the daily points fell into a group of regular patterns when plotting discharge against water level. The data present significant stratification phenomena, especially in low and normal flow scenarios. Further, rating curves that describe the relationship between discharge and stage for the 27 groups of data sets derived based on ANN are shown in Figure 4.

The rating curves established for different phases demonstrate significant and sudden shifts in each scenario.

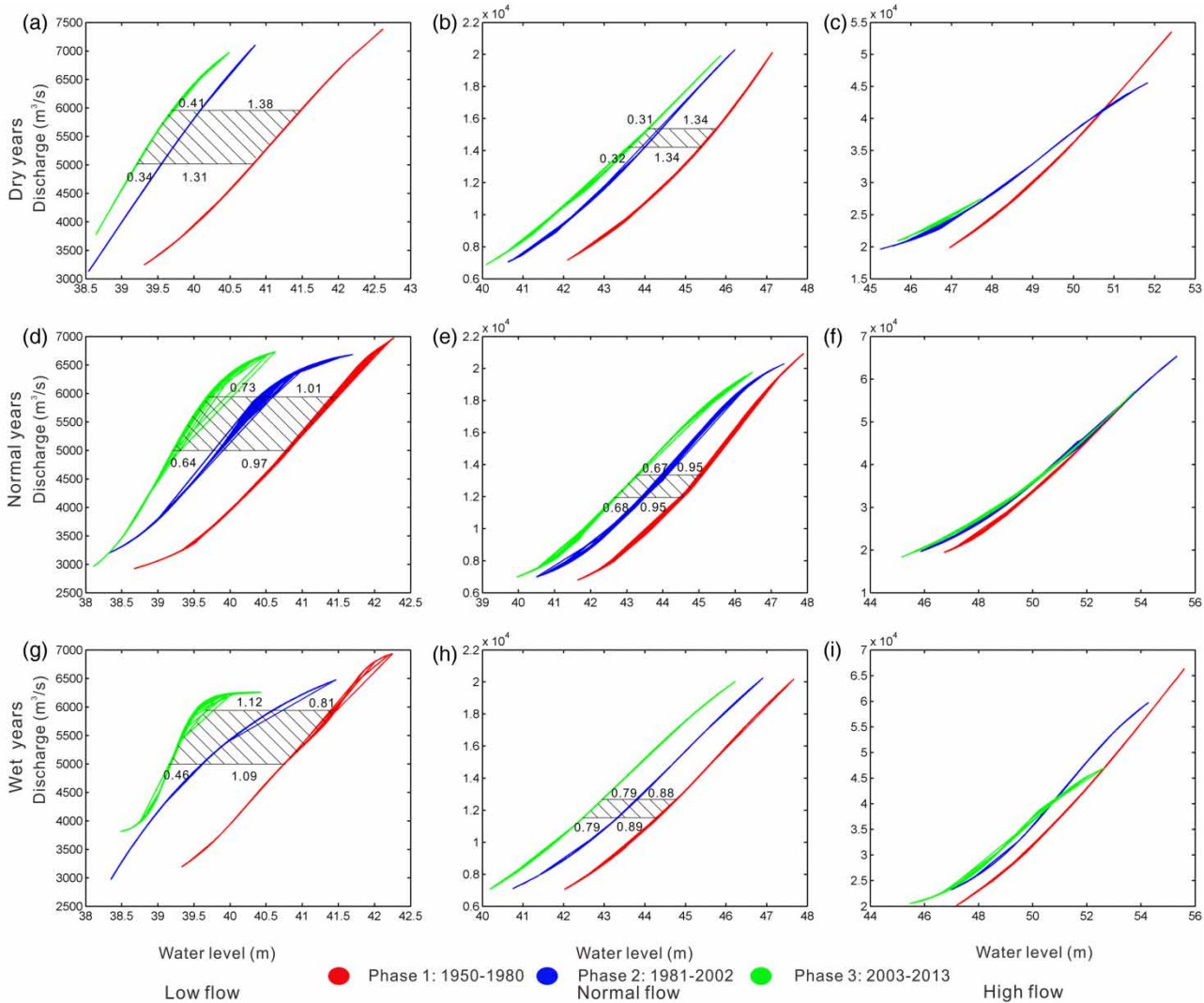


**Figure 4** | Stage–discharge rating curves for Yichang hydrometric station.

It is shown that the obtained curves present upgrade tendencies since GD and TGD were put into practice. The rating curves of Phase 3 lie on the top of the plots. However, the tendencies do not appear to be the same for all sets. Details are as follows.

### Normal flow

The rating curves in the normal flow scenario indicate equilibrium state with almost the same slopes (Figure 4(b), 4(e), and 4(h)). In this case, the rating curves of Phase 3 and Phase 2 are relatively parallel to the one under natural conditions. For different amounts of discharge, the net differences between

Phase 1 and Phase 2 are stable at 1.34 m, 0.95 m, and 0.88 m in dry year, normal year, and wet year, respectively. On the other hand, the calculated differences between Phase 2 and Phase 3 corresponding to dry year, normal year, and wet year are around 0.31 m, 0.67 m, and 0.79 m, respectively. Obviously, the variations between Phase 1 and Phase 2 show a decreasing trend while that between Phase 2 and Phase 3 display an upward trend with annual discharge.

### Low flow

In the low flow scenario, the intercepts between Phase 1 and Phase 2, Phase 2 and Phase 3 are variable at different



discharge level. In real terms, at 5,000 m<sup>3</sup>/s discharge level, GD induces 1.31 m, 0.97 m, and 1.09 m reduction of water level in dry years, normal years, and wet years, respectively, while TGD results in 0.34, 0.64, and 0.46 m of water level decline (Figure 2(a), 2(d), and 2(g)). When discharge increases to 6,500 m<sup>3</sup>/s, the water level differences between Phase 1 and Phase 2 in dry years, normal years, and wet years are 1.38, 1.01, and 0.81 m while those between Phase 2 and Phase 3 are 0.41, 0.73, and 1.12 m (Figure 2(a), 2(d), and 2(g)).

### High flow

The high flow scenario is characterized by mixed rating curves at intersection points. For the present study, the water level difference with respect to different amounts of discharges between Phase 1, Phase 2, and Phase 3 are random without order and can present either a positive or negative value. Specifically, in dry years, the curves of Phase 1 and Phase 2 converge at around 42,700 m<sup>3</sup>/s (Figure 4(c)). In normal years, the curve of Phase 3 goes across that of Phase 2 and Phase 1 at about 42,700 m<sup>3</sup>/s and 52,200 m<sup>3</sup>/s, respectively (Figure 4(f)). In wet years, the curves of Phase 2 and Phase 3 intersect at around 42,100 m<sup>3</sup>/s (Figure 4(i)).

Taken altogether, the rating curves constructed at different phases present significant upward shifts for low and normal flow scenarios, indicating that water level becomes lower corresponding to the same amount of discharge. On the other hand, rating curves for high flow scenario have no regular pattern. It is noted that the rating curves for both low and high flow scenarios present hysteretic behaviors.

## DISCUSSION

The variations of stage–discharge relationships can be explained by changes in river discharge as well as water level. Here, precipitation, dam regulation, sand exploitation, and channel erosion, the possible indicators that may affect the relations between water level and discharge are discussed.

### Regional precipitation

Precipitation is the dominant factor that controls the runoff within the upper Yangtze River basin (Wang et al. 2013b). Therefore, variations in river discharge are likely to be consistent with that of precipitation in natural hydrological conditions. Regional precipitation over the upper Yangtze River that controls the discharge of Yichang station is calculated by Thiessen polygon method, as shown in Figure 5. It is shown that the seasonal rainfall over the upper Yangtze River indicates decreasing trends in summer, autumn, and winter, but a rising trend in spring over the period of 1960–2013. In contrast to the significant changes in river discharge, the seasonal precipitation series only suggest slight change. Hence, precipitation cannot explain the substantial discharge variations in Yichang station over the past half century.

### Dam regulation

Generally, a dam tends to stabilize the low flows and eliminate the high flows (Magilligan et al. 2003; Graf 2006). For unsteady flows, the relationship between discharge and water level is looped rating curve, or hysteretic curve (Petersen-Overleir 2006). As Figure 4 indicates, the rating curves for low flow scenario present strong hysteretic behaviors, which mainly occurred in April and May (Mei et al. 2015). The middle and lower reaches of the Yangtze River are affected by spring droughts (from April to May) and

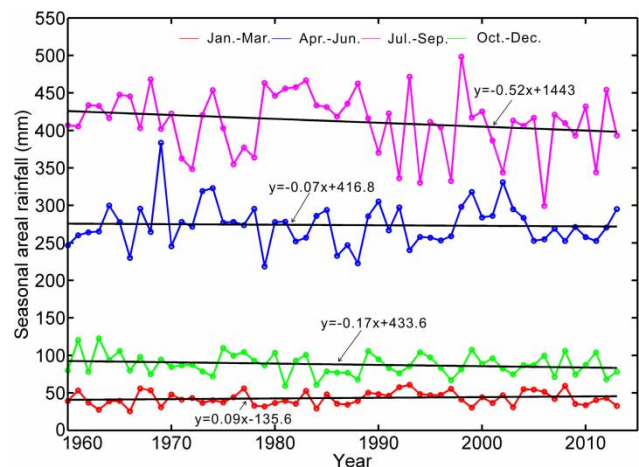


Figure 5 | Seasonal areal precipitation over the upper Yangtze River.

summer floods (from June to September); the upper stream GD and TGD, especially TGD, therefore release water during spring to ease downstream droughts as well as prepare storage for the coming floods. Thereafter, the reservoirs controlled water release in April and May reverse the natural flow regime downstream by mitigating the variations in discharge and water level, which results in looped rating curves in the low flow scenario. Meanwhile, as for the hysteresis phenomenon of rating curves in high flow, it is a result of backwater effect associated with flood wave propagation (Wolfs & Willems 2014). Here, the annual discharge series are divided into three sub-series according to dam constructions, and their mean values are examined (Figure 6(a)–6(c)). It is demonstrated that annual maximum hydrology events are concentrated in June and July (84%) while annual minimum events are mainly located between February and March (81%). GD suggests slight influence on river discharge. Conversely,  $Q_{\min}$ ,  $Q_{\text{mean}}$ , and  $Q_{\text{max}}$  present significant changes when TGD starts to work. Specifically, the mean value of  $Q_{\min}$  increased by 31.14% (from 3,427 to 4,494  $\text{m}^3/\text{s}$ ), while the average

$Q_{\text{mean}}$  and average  $Q_{\text{max}}$  dropped by 10.06% (from 13,791 to 12,404  $\text{m}^3/\text{s}$ ) and 16.35% (from 50,210 to 42,003  $\text{m}^3/\text{s}$ ), respectively, with the impact of TGD (Figure 6(a)–6(c)). The different performances of GD and TGD on annual discharge can be explained by their storage capacities and dam functions. As mentioned in Table 1, the capacity of GD is 1,580 million  $\text{m}^3$  whereas the storage of TGD is nearly 25 times that of GD. Moreover, GD was built as a re-regulation reservoir while TGD was designed partly for flood control. Consequently, the effect of GD on river discharge in the period from 1950 to 2013 is negligible. The great variations of discharge at Yichang station mainly result from TGD regulation.

### Sand exploitation and channel erosion

For a stable cross section, the variation of water level is likely to follow that of discharge. However, in this study, the patterns of water level series are significantly different from that of discharge. For instance, during GD regulation period (1981–2002), the water levels dramatically reduced whereas

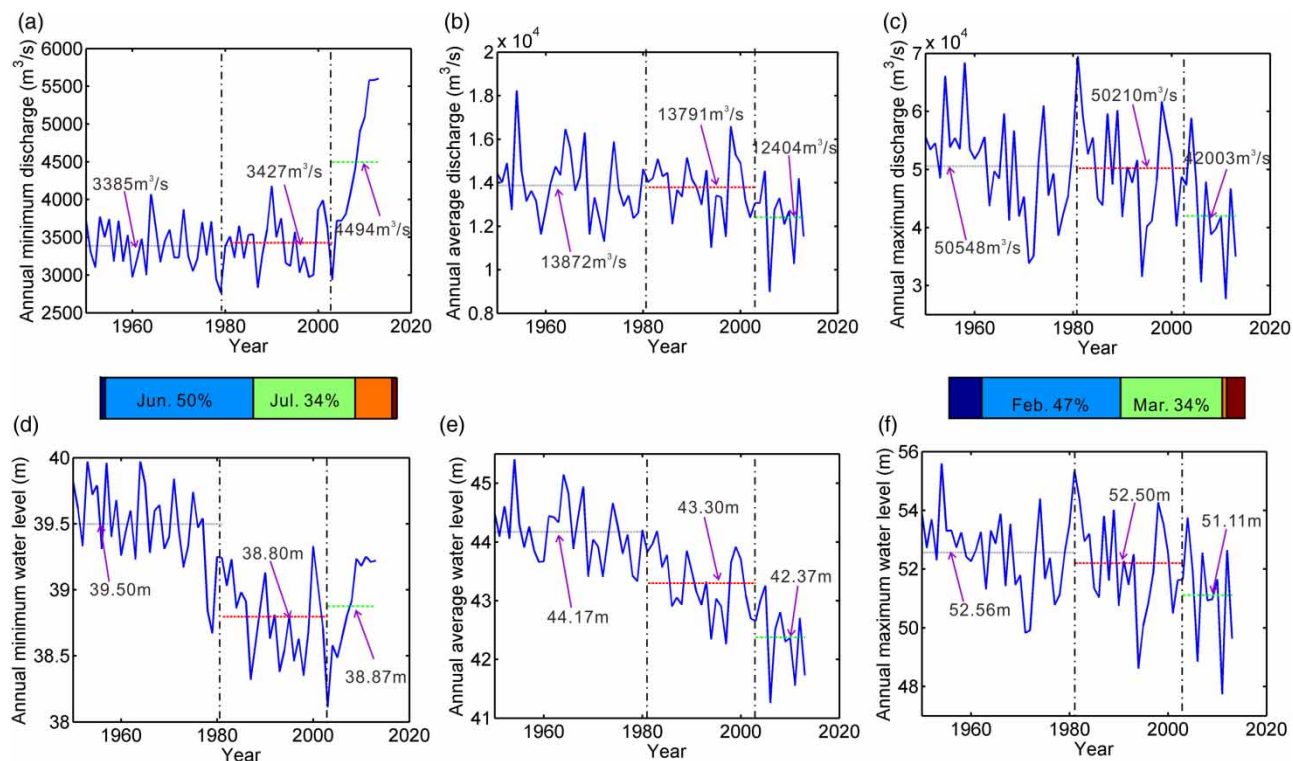


Figure 6 | Annual discharge and water level series with mean values.

the river discharge was relatively stable (Figure 6(d)–6(f)). The variation in riverbed morphology at Yichang station is a possible reason for this phenomenon, which can be caused in two ways: sand exploitation and channel erosion.

According to Rao et al. (1999), around 10.5 million m<sup>3</sup> bed material (sand and gravel) was exploited from Zhenchuanmen to Huyatan, a 17.94 km stretch below GD, for the construction of GD over the period 1972–1981, which resulted in significant riverbed degradation. Sand mining continued until 1987, when another 14.26 million m<sup>3</sup> of bed material was exploited.

When the upstream reservoirs started to impound water and trap sediment, the riverbed morphology at Yichang station was further changed in terms of bed erosion. Over the past century, the annual sediment loads at Yichang indicate dramatic reductions following the construction of GD and TGD (Figure 7). Compared to GD, TGD induced a much stronger effect on downstream sediment loads due to larger storage capacity. From 2003 to 2008, TGD caused 172 million tons of annual sediment deposition in the upper reaches from Pingshan to Yichang and 4.4 million tons of annual sediment erosion between the site of TGD and Yichang (Hu et al. 2009).

### Distinguishing the effect of sand exploitation, GD regulation, and TGD regulation on rating curve variations

River incision is a main cause of stage–discharge variation at Yichang station (Rao et al. 1999; Wang et al. 2013a).

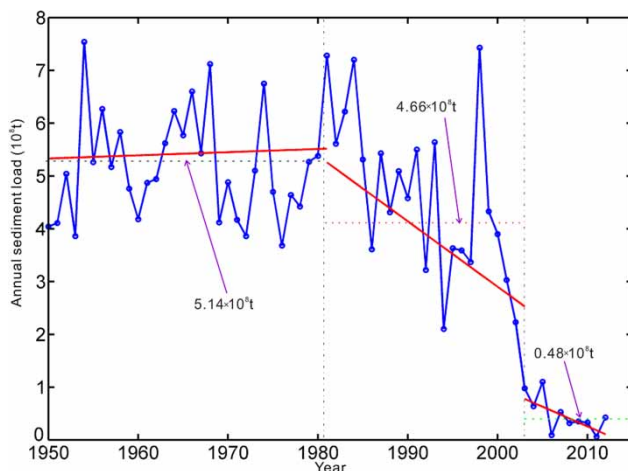


Figure 7 | Annual sediment load at Yichang station.

Therefore, it is necessary to quantify the morphology evolution of Yichang cross section during the past five decades (Figure 8). It is shown that the greatest geomorphologic change occurs in the central portion of the cross section (between 200 and 800 m from the left bank). At the beginning of the 1970s, Yichang cross section was characterized as a V shape, which changed to a W shape between 1981 and 2002, after which it took the form of a U shape. Meanwhile, significant erosion was observed. The total scoured depth at 600 m from the left bank for the Yichang cross section is around 4 m. Specifically, the bed elevation decreased from 24.3 to 23.5 m (degraded 0.8 m) over the period 1970–1981, and then exhibited more than a 10% decrease between 1981 and 1987 (from 23.5 to 21.1 m). Bed erosion continued in the following years, with the bed elevation decreasing to 20.8 m and 20.4 m in 2002 and 2012, respectively. In addition, the deepest riverbed moved toward the left bank continuously, with a swing distance around 90 m.

As Figure 8 indicates, channel erosion at Yichang cross section mainly occurs in the area below 45 m bed elevation, which corresponds to the high flow scenario. Therefore, water levels corresponding to 20,000 m<sup>3</sup>/s at different time periods are calculated to distinguish the impacts of various anthropogenic activities on rating curves (Table 5). Over the past five decades, the water level under the 20,000 m<sup>3</sup>/s scenario presented 2.01 m degradation (from 47.39 to 45.38 m). From 1972 to 1981, the changes in cross section were fully due to sand mining, which led to a 0.31 m water level decrease. In the following 6 years (from 1981

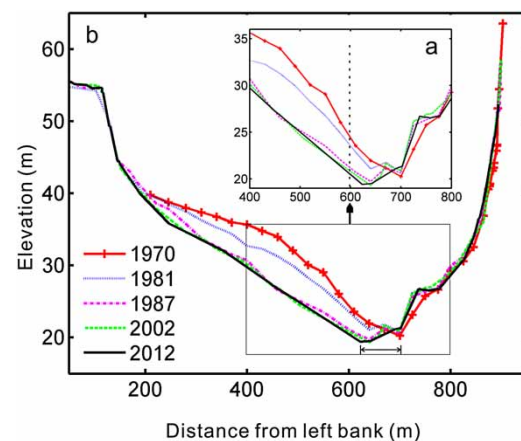


Figure 8 | Evolution of Yichang cross section from 1970 to 2012.

**Table 5** | Quantification of human activities on bed erosion at Yichang station for high flow scenario (20,000 m<sup>3</sup>/s)

Year	Water level	Human activity	Water level reduction	Contribution (%)
1972–1981	47.39–47.08	Sand mining	0.31	36
1981–1987	47.08–46.51	Sand mining	0.42	11
		GD regulation	0.15	
1987–2003	46.51–46.45	GD regulation	0.06	
2003–2013	46.45–45.38	TGD regulation	1.07	53

to 1987), Yichang cross section experienced both sand mining and dam regulation, and presented a 0.57 m water level reduction. From 2002 to 2012, TGD regulation was the main reason for bed elevation scour, which resulted in 1.07 m of water level decrease. To distinguish the effects of sand mining and GD regulation on riverbed incision during 1981–1987, this study assumes that sand mining from 1981 to 1987 occurred at the same place with the same mining patterns as that of 1972–1981. Therefore, sand mining-induced water level change during 1981–1987 can be estimated based on the ratio of sand mining quantity over the two periods and the water level decrease between 1972 and 1981. During the study period, Yichang cross section experienced 2.01 m bed erosion with respect to 20,000 m<sup>3</sup>/s discharge. The relative contributions of sand mining, GD, and TGD amount to 36%, 53%, and 11%, respectively (Table 5).

## CONCLUSIONS

The upper Yangtze River is characterized by intensive river engineering. In addition to the course of climate change, it is valuable to assess the influence of dam regulation on river stage-discharge relationships. This study focuses on the rating curve variations at Yichang station, the first control station downstream of GD and TGD reservoirs. The main findings are summarized as follows:

1. There are clear abrupt changes around 1981 and 2003 for water level and discharge at Yichang station when GD and TGD were constructed. Meanwhile, from 1950 to 2013, annual maximum and mean discharge, annual maximum, mean and minimum water level show

decreasing trends while annual minimum discharge presents an upward trend.

2. The long-term relationship of stage to discharge is drastically altered by human activities over the period 1950–2013, and can be classified into the following three types: (a) normal flow: the rating curves present similar slopes and reach equilibrium state; (b) low flow: the reduction in water level changes with water discharge; and (c) high flow: the rating curves cross each other without observable regularity.
3. Sand mining, GD regulation, and TGD regulation are responsible for rating curve variations at Yichang station. Among them, TGD regulation is the leading cause (53%), sand mining is second (36%), and GD regulation has the smallest effect (11%).

## ACKNOWLEDGEMENTS

This study is supported by the Ministry of Science and Technology of China (SKLEC: 2010RCDW03) and NSFC (41076050). We are grateful to Editor Chong-Yu Xu and two anonymous reviewers for their constructive comments and suggestions that improved the article.

## REFERENCES

- Al-Abadi, A. 2014 Modeling of stage-discharge relationship for Gharraf River, southern Iraq using backpropagation artificial neural networks, M5 decision trees, and Takagi-Sugeno inference system technique: a comparative study. *Appl. Water Sci.* 1–14, doi: 10.1007/s13201-014-0258-7.
- Birkhead, A. L. & James, C. S. 1998 Synthesis of rating curves from local stage and remote discharge monitoring using nonlinear Muskingum routing. *J. Hydrol.* **205**, 52–65.
- Bourquin, J., Schmidli, H., van Hoogevest, P. & Leuenberger, H. 1998 Advantages of artificial neural networks (ANNs) as alternative modeling technique for data sets showing non-linear relationships using data from a galenic study on a solid dosage form. *Eur. J. Pharm. Sci.* **7** (1), 5–16.
- Chen, Z., Gupta, A. & Yin, H. F. (eds) 2007 Large monsoon rivers of Asia. *Geomorphology (Special Issue)* **85** (3–4), 316.
- Chen, Y. D., Zhang, Q., Xu, C. Y., Yang, T., Chen, X. H. & Jiang, T. 2009 Change-point alterations of extreme water levels and underlying causes in the Pearl River Delta, China. *River Res. Appl.* **25**, 1153–1168.

- Dai, Z. J. & Liu, J. T. 2013 Impacts of large dams on downstream fluvial sedimentation: an example of the Three Gorges Dam (TGD) on the Changjiang (Yangtze River). *J. Hydrol.* **480**, 10–18.
- Dai, A., Trenberth, K. E. & Karl, T. R. 1998 Global variations in droughts and wet spells: 1900–1995. *Geophys. Res. Lett.* **25** (17), 3367–3370.
- Dai, Z. J., Du, J., Li, J., Li, W. & Chen, J. 2008 Runoff characteristics of the Changjiang River during 2006: effect of extreme drought and the impounding of the Three Gorges Dam. *Geophys. Res. Lett.* **35**, L07406.
- Dai, Z. J., Chu, A., Du, J., Stive, M. & Yan, H. 2010 Assessment of extreme drought and human interference on baseflow of the Yangtze River. *Hydrol. Process.* **24**, 749–757.
- Dai, Z. J., Liu, J. T. & Xiang, Y. B. 2014 Human interference in the water discharge of the Changjiang (Yangtze River), China. *Hydrolog. Sci. J.* doi:10.1080/02626667.2014.944182.
- Dettinger, M. D. & Diaz, H. F. 2000 Global characteristics of stream flow seasonality and variability. *J. Hydrometeorol.* **1**, 289–310.
- Fielder, F. R. 2003 Simple, practical method for determining station weights using Thiessen polygons and isohyetal maps. *J. Hydrol. Eng.* **8** (4), 219–221.
- Gordon, E. & Meentemeyer, R. K. 2006 Effects of dam operation and land use on stream channel morphology and riparian vegetation. *Geomorphology* **82**, 412–429.
- Graf, W. L. 2006 Downstream hydrologic and geomorphic effects of large dams on American rivers. *Geomorphology* **79** (3–4), 336–360.
- Güven, A. & Aytekin, A. 2009 New approach for stage–discharge relationship: gene-expression programming. *J. Hydrol. Eng.* **14** (8), 812–820.
- Hsu, K., Gupta, H. V. & Sorooshian, S. 1995 Artificial neural network modeling of the rainfall-runoff process. *Water Resour. Res.* **31** (10), 2517–2530.
- Hu, B. Q., Yang, Z. S., Wang, H. J., Sun, X. X., Bi, N. S. & Li, G. G. 2009 Sedimentation in the Three Gorges Dam and the future trend of Changjiang (Yangtze River) sediment flux to the sea. *Hydrol. Earth Syst. Sci.* **13**, 2253–2264.
- Jain, S. K. & Chalisgaonkar, D. 2000 Setting up stage discharge relations using ANN. *J. Hydrol. Eng.* **5** (4), 428–433.
- Jiang, S. H., Ren, L. L., Yong, B., Singh, V. P., Yang, X. L. & Yuan, F. 2011 Quantifying the effects of climate variability and human activities on runoff from the Laohahe basin in northern China using three different methods. *Hydrol. Process.* **25**, 2492–2505.
- Khalique, M. N. & Ouarda, T. B. M. J. 2007 Short communication on the critical values of the standard normal homogeneity test (SNHT). *Int. J. Climatol.* **27**, 681–687.
- Kisi, O. & Cobaner, M. 2009 Modeling river stage-discharge relationships using different neural network computing techniques. *Clean Soil Air Water* **37** (2), 160–169.
- Labat, D., Godderis, Y., Probst, J. L. & Guyot, J. L. 2004 Evidence for global runoff increase related to climate warming. *Adv. Water Resour.* **27**, 631–642.
- Lloyd-Hughes, B. & Saunders, M. A. 2002 A drought climatology for Europe. *Int. J. Climatol.* **22**, 1571–1592.
- Lu, X. X. 2005 Spatial variability and temporal change of water discharge and sediment flux in the lower Jinsha tributary: impact of environmental changes. *River Res. Appl.* **21**, 229–243.
- Magilligan, F. G., Nislow, K. H. & Graber, B. E. 2003 Scale-independent assessment of discharge reduction and riparian disconnectivity following flow regulation by dams. *Geology* **31**, 569–572.
- McManamay, R. A. 2014 Quantifying and generalizing hydrologic responses to dam regulation using a statistical modeling approach. *J. Hydrol.* **519**, 1278–1296.
- Mei, X., Dai, Z., van Gelder, P. H. A. J. M. & Gao, J. 2015 Linking Three Gorges Dam and downstream hydrological regimes along the Yangtze River, China. *Earth Space Sci.* **2**, 1–13.
- Milliman, J. D., Farnsworth, K. L., Jones, P. D., Xu, K. H. & Smith, L. C. 2008 Climatic and anthropogenic factors affecting river discharge to the global ocean, 1951–2000. *Global Planet. Change* **62**, 187–194.
- Milly, P. C. D., Dunne, K. A. & Vecchia, A. V. 2005 Global pattern of trends in streamflow and water availability in a changing climate. *Nature* **438** (1), 347–350.
- Ministry of Water Resources of the People's Republic of China. (MWR) 2013 *Bulletin of first national census for water*. [http://www.irtces.org/isi/isi\\_document/2013/bulletin/FirstCensusWater.pdf](http://www.irtces.org/isi/isi_document/2013/bulletin/FirstCensusWater.pdf).
- Moyeed, R. A. & Clarke, R. T. 2005 The use of Bayesian methods for fitting rating curves, with case studies. *Adv. Water Resour.* **28**, 807–818.
- Naik, P. K. & Jay, D. A. 2011 Human and climate impacts on Columbia River hydrology and salmonids. *River Res. Appl.* **27**, 1270–1276.
- Perumal, M., Shrestha, K. & Chaube, U. 2004 Reproduction of hysteresis in rating curves. *J. Hydrol. Eng.* **130** (9), 870–878.
- Petersen-Øverleir, A. 2006 Modelling stage–discharge relationships affected by hysteresis using the Jones formula and nonlinear regression. *Hydrol. Sci. J.* **51** (3), 365–388.
- Rao, G. S., Sun, E. Y. & Li, F. Z. 1999 Cause analysis and countermeasures of water level drop downstream Gezhouba project. *Yangtze River* **30** (9), 28–30 (in Chinese).
- Rojas, R. 1996 *Neural Networks: A Systematic Introduction*. Springer-Verlag, Berlin.
- Shin, Y. H. 2007 Channel changes downstream of the Hapcheon Re-regulation Dam in South Korea. Dissertation (PhD), Colorado State University, Fort Collins, CO.
- Shrestha, R. R. & Simonovic, S. P. 2010 Fuzzy nonlinear regression approach to stage-discharge analyses: case study. *J. Hydrol. Eng.* **15** (1), 49–56.
- Snee, R. D. 1977 Validation of regression models: methods and examples. *Technometrics* **19** (4), 415–428.
- Sudheer, K. & Jain, S. 2003 Radial basis function neural network for modeling rating curves. *J. Hydrologic Eng.* **8** (3), 161–164.
- Talebizadeh, M., Morid, S., Ayyoubzadeh, S. A. & Ghasemzadeh, M. 2009 Uncertainty analysis in sediment load modeling

- using ANN and SWAT model. *Water Resour. Manage.* **24** (9), 1747–1761.
- Tawfik, M., Ibrahim, A. & Fahmy, H. 1997 Hysteresis sensitive neural network for modeling rating curves. *J. Comput. Civ. Eng.* **11** (3), 206–211.
- Wang, J. D., Sheng, Y. W., Gleason, C. J. & Wada, Y. 2013a Downstream Yangtze River levels impacted by Three Gorges Dam. *Environ. Res. Lett.* **8**, 044012.
- Wang, W. G., Xing, W. Q., Yang, T., Shao, Q. X., Peng, S. Z., Yu, Z. B. & Yong, B. 2013b Characterizing the changing behaviours of precipitation concentration in the Yangtze River Basin, China. *Hydrol. Process.* **27**, 3375–3393.
- Wolfs, V. & Willems, P. 2014 Development of discharge-stage curves affected by hysteresis using time varying models, model trees and neural networks. *Environ. Modell. Softw.* **55**, 107–119.
- Xu, K. H. & Milliman, J. D. 2009 Seasonal variations of sediment discharge from the Yangtze River before and after impoundment of the Three Gorges Dam. *Geomorphology* **104**, 276–283.
- Xu, C. Y., Gong, L., Jiang, T., Chen, D. & Singh, V. P. 2006a Analysis of spatial distribution and temporal trend of reference evapotranspiration and pan evaporation in Changjiang (Yangtze River) catchment. *J. Hydrol.* **327** (1–2), 81–93.
- Xu, K. H., Milliman, J. D., Yang, Z. S. & Wang, H. J. 2006b Yangtze sediment decline partly from Three Gorges Dam. *EOS Trans.* **87** (19), 185–190.
- Xu, J. J., Yang, D. W., Lei, Z. D., Chen, J. & Yang, W. J. 2008 Spatial and temporal variation of runoff in the Yangtze River basin during the past 40 years. *Quatern. Int.* **186**, 32–42.
- Yang, Y. H. & Tian, F. 2009 Abrupt change of runoff and its major driving factors in Haihe River Catchment, China. *J. Hydrol.* **374**, 373–383.
- Yang, S. L., Zhang, J., Zhu, J., Smith, J. P., Dai, S. B., Gao, A. & Li, P. 2005 Impact of dams on Yangtze River sediment supply to the sea and delta intertidal wetland response. *J. Geophys. Res.* **110**, F03006.
- Yang, Z. S., Wang, H. J., Saito, Y., Milliman, J. D., Xu, K. H., Qiao, S. Q. & Shi, G. Y. 2006 Dam impacts on the Changjiang (Yangtze) River sediment discharge to the sea: the past 55 years and after the Three Gorges Dam. *Water Resour. Res.* **42**, W04407.
- Yang, S. L., Zhang, J., Dai, S. B., Li, M. & Xu, X. J. 2007 Effect of deposition and erosion within the main river channel and large lakes on sediment delivery to the estuary of the Yangtze River. *J. Geophys. Res.* **112**, F02005.
- Yue, S., Pilon, P. J., Phinney, B. & Cavadias, G. 2002 The influence of autocorrelation on the ability to detect trend in hydrological series. *Hydrol. Process.* **16**, 1807–1829.
- Zhang, Q., Liu, C. L., Xu, C. Y., Xu, Y. P. & Jiang, T. 2006a Observed trends of annual maximum water level and streamflow during past 130 years in the Yangtze River basin, China. *J. Hydrol.* **324**, 255–265.
- Zhang, Q., Xu, C. Y., Becker, S. & Jiang, T. 2006b Sediment and runoff changes in the Yangtze River basin during past 50 years. *J. Hydrol.* **331**, 511–523.
- Zhang, Q., Xu, C. Y., Zhang, Z., Chen, Y. D., Liu, C. L. & Lin, H. 2008a Spatial and temporal variability of precipitation maxima during 1960–2005 in the Yangtze River basin and possible association with large-scale circulation. *J. Hydrol.* **353**, 215–227.
- Zhang, Q., Xu, C. Y., Chen, Y. Q., Gemmer, M. & Yu, Z. G. 2008b Multifractal detrended fluctuation analysis of streamflow series of the Yangtze River basin, China. *Hydrol. Process.* **22**, 4997–5003.
- Zhang, Y. Y., Arthington, A. H., Bunn, S. E., Mackay, S., Xia, J. & Kennard, M. 2012 Classification of flow regimes for environmental flow assessment in regulated rivers: the Huai River Basin, China. *River Res. Appl.* **28**, 989–1005.
- Zhang, W., Wang, W. G., Zheng, J. H., Wang, H. G., Wang, G. & Zhang, J. S. 2015 Reconstruction of stage-discharge relationships and analysis of hydraulic geometry variations: the case study of the Pearl River Delta, China. *Global Planet. Change* **125**, 60–70.
- Zhao, G. J., Mu, X. M., Tian, P., Wang, F. & Gao, P. 2013 Climate changes and their impacts on water resources in semiarid regions: a case study of the Wei River basin, China. *Hydrol. Process.* **27**, 3852–3863.

First received 13 January 2015; accepted in revised form 25 April 2015. Available online 6 June 2015